ORIGINAL PAPER

Nagoya J. Med. Sci. **82**. 261–280, 2020
doi:10.18999/nagjms.82.2.261

# Vaticanol C, a phytoalexin, induces apoptosis of leukemia and cancer cells by modulating expression of multiple sphingolipid metabolic enzymes

Chisato Inoue[1], Sayaka Sobue[1], Naoki Mizutani[1], Yoshiyuki Kawamoto[1], Yuji Nishizawa[1], Masatoshi Ichihara[1], Toshiyuki Takeuchi[2], Fumihiko Hayakawa[3], Motoshi Suzuki[2], Tetsuro Ito[4,5], Yoshinori Nozawa[6], and Takashi Murate[1]

[1]*College of Life and Health Sciences, Chubu University, Kasugai, Japan*
[2]*Department of Molecular Oncology, Fujita Health University, Toyoake, Japan*
[3]*Department of Medical Technology, Nagoya University Graduate School of Health Sciences, Nagoya, Japan*
[4]*Gifu Pharmaceutical University, Gifu, Japan*
[5]*Gifu Prefectural Research Institute for Health and Environmental Sciences, Kakamigahara, Japan*
[6]*Tokai Gakuin University, Kakamigahara, Japan*

## ABSTRACT

Resveratrol (RSV) has recently attracted keen interest because of its pleiotropic effects. It exerts a wide range of health-promoting effects. In addition to health-promoting effects, RSV possesses anti-carcinogenic activity. However, a non-physiological concentration is needed to achieve an anti-cancer effect, and its *in vivo* bioavailability is low. Therefore, the clinical application of phytochemicals requires alternative candidates that induce the desired effects at a lower concentration and with increased bioavailability. We previously reported a low $IC_{50}$ of vaticanol C (VTC), an RSV tetramer, among 12 RSV derivatives (Ito T. et al, 2003). However, the precise mechanism involved remains to be determined. Here, we screened an in-house chemical library bearing RSV building blocks ranging from dimers to octamers for cytotoxic effects in several leukemia and cancer cell lines and their anti-cancer drug-resistant sublines. Among the compounds, VTC exhibited the highest cytotoxicity, which was partially inhibited by a caspase 3 inhibitor, Z-VAD-FMK. VTC decreased the expression of sphingosine kinase 1, sphingosine kinase 2 and glucosylceramide synthase by transcriptional or post-transcriptional mechanisms, and increased cellular ceramides/dihydroceramides and decreased sphingosine 1-phosphate (S1P). VTC-induced sphingolipid rheostat modulation (the ratio of ceramide/S1P) is thought to be involved in cellular apoptosis. Indeed, exogenous S1P addition modulated VTC cytotoxicity significantly. A combination of SPHK1, SPHK2, and GCS chemical inhibitors induced sphingolipid rheostat modulation, cell growth suppression, and cytotoxicity similar to that of VTC. These results suggest the involvement of sphingolipid metabolism in VTC-induced cytotoxicity, and indicate VTC is a promising prototype for translational research.

Keywords: vaticanol C, apoptosis, sphingolipid rheostat, SPHK, GCS

Abbreviations:
RSV: resveratrol
VTC: vaticanol C
ADR: Adriamycin
ASMase: acid sphingomyelinase
NSMase: neutral sphingomyelinase

Received: August 2, 2019; accepted: October 1, 2019

Corresponding Author: Takashi Murate, MD, PhD
College of Life and Health Sciences, Chubu University, Matsumoto-cho 1200, Kasugai, Aichi 487-8501, Japan
Tel: +81-568-51-9547, E-mail: murate@isc.chubu.ac.jp

ACDase: acid ceramidase
SPHK: sphingosine kinase
SPL: sphingosine 1-phosphate lyase
GCS: glucosylceramide synthase
CERS: ceramide synthase
DES1: dihydroceramide desaturase
LC-MS/MS: liquid chromatography-tandem mass spectrometry
S1P: sphingosine 1-phosphate
Ph+ALL: Philadelphia chromosome positive acute lymphoblastic leukemia
PDMP: *N*-[2-hydroxyl-1-(4-monopholinylmethyl)-2-phenylethyl]-decanamide



## INTRODUCTION

Resveratrol (RSV) is a plant-derived polyphenolic phytoalexin, which exerts a wide range of health-promoting effects.[1] RSV has antioxidant and anti-inflammatory activities, and has been reported to activate the sirtuin NAD-dependent histone deacetylase.[2] In addition to these health-promoting effects, RSV possesses anti-carcinogenic activity.[1,3] Subsequent studies demonstrated the clinical utility of RSV as an anti-cancer drug. The pleiotropic effects of RSV are dependent on its concentration and sometimes the cell context. For example, RSV exhibited pro-oxidant properties in the presence of transition metal ions and mediated DNA cleavage.[4] At low doses it exhibited cell protection, and at high doses it induced cytotoxicity and a DNA-damaging effect, referred to as the hormesis effect.

Sphingolipids are important for maintaining the barrier function and fluidity of cell membranes. Moreover, sphingolipids, especially ceramide and S1P, are regarded as important intra- and inter-cellular signaling molecules that regulate cell growth, proliferation, death, and migration.[5] The sphingolipid rheostat model (the ratio of ceramide/S1P) has been proposed to explain the above-described phenomena,[6] and its adequacy has recently been proven in many *in vitro* and *in vivo* models.

We have recently reported RSV-induced acid sphingomyelinase (ASMase) mRNA expression of a human leukemia cell line, K562, and that its enzyme activity led to ceramide accumulation.[7] RSV exhibits strong cell growth inhibitory activity, but a high concentration (100 μM) is needed for this effect. In addition, RSV has poor bioavailability *in vivo*. Therefore, a new strategy is required to resolve this issue. The development of ideal RSV analogs is highly desired. We reported that a RSV tetramer, vaticanol C (VTC), at a low concentration was more effective at inducing cancer cell apoptosis than RSV.[8] However, the precise cytotoxic mechanism of VTC remains to be determined.

Here, cytotoxicities of RSV and its oligomers were examined in various leukemia and cancer cell lines. Among the analyzed RSV derivatives, VTC exhibited the strongest cytotoxic activity. VTC increased cellular ceramide and dihydroceramide, and decreased S1P. Interestingly, VTC was not effective at inducing ASMase enzyme activity in contrast to our recent report of RSV,[7] while the downregulation of sphingosine kinase 1 and 2 (SPHK1 and SPHK2) and glucosylceramide synthase (GCS) was observed with VTC. Thus, we focused on these enzymes and examined their relevance to VTC-induced apoptosis. Chemical inhibitors of SPHK1, SPHK2, and GCS suppressed cell proliferation and viability (especially in combination) of the tested cell lines, which were very similar to VTC. The involvement of these enzymes in malignant cells for survival and anti-apoptotic effects was examined.

## MATERIALS AND METHODS

*Cell lines*

Human erythroleukemia cell line K562, its adriamycin (ADR)-resistant subclone K562/ADR, human prostate cancer cell line PC3, and its paclitaxel-resistant subclone PC3-PR have been described previously.[9,10] The Philadelphia chromosome positive acute lymphoblastic leukemia (Ph+ALL) cell line NphA2 and its imatinib-resistant subclone NphA2/STIR, were reported recently.[11] Other leukemia cell lines, BALL1, NALL1, Jurkat, and U937, have been described before.[12]

*Resveratrol oligomer*

Resveratrol oligomers (four dimers, one trimer, eight tetramers, and one octamer) were purified according to a previously described method.[8]

*Reagents*

RSV, N-acetyl-L-cysteine (NAC), sulforaphane, curcumin, and quercetin were purchased from Sigma-Aldrich (St. Louis, MO, USA). Epigallocatechin gallate (EGCG) was purchased from Funakoshi Co. (Tokyo, Japan). Z-VAD-FMK, a pan-caspase inhibitor, was purchased from Promega (Madison, WI, USA). SPHK1 inhibitor SKI-II (described as SKI in the text), SPHK2 inhibitor ABC294640, GCS inhibitor PDMP, and sphingosine 1-phosphate (S1P) were purchased from Cayman Chemical (Ann Arbor, MI, USA). GT-11,[13] a dihydroceramide desaturase (DES1) inhibitor, was obtained from Avanti Polar Lipids, Inc. (Alabaster, AL, USA).

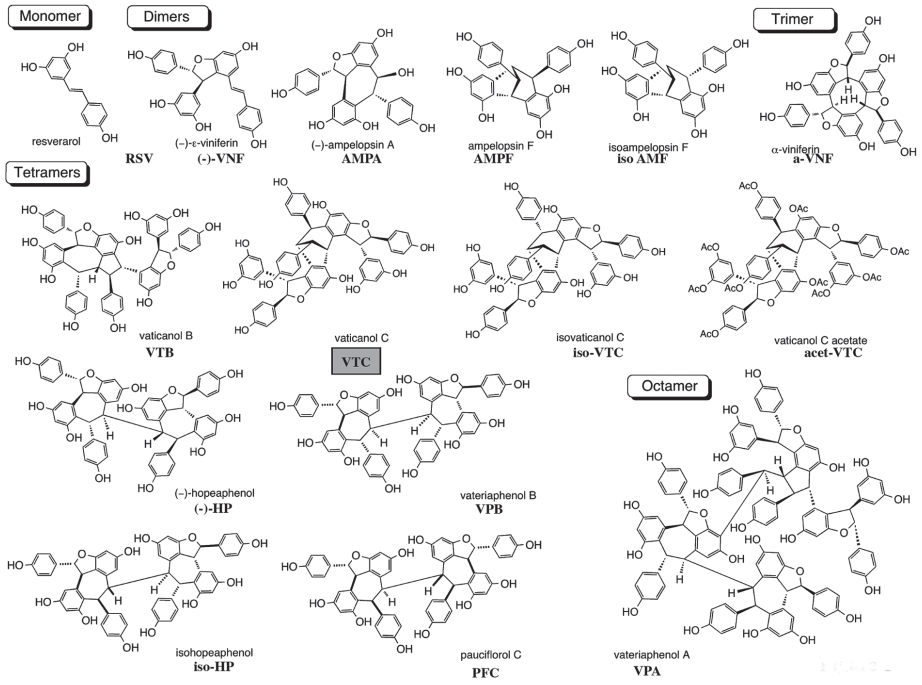


**Fig. 1** RSV and its oligomers

Chemical structures of resveratrol (RSV) and its oligomers (4 dimers, 1 trimer, and 8 tetramers and 1 octamer) are shown. VTC was boxed.

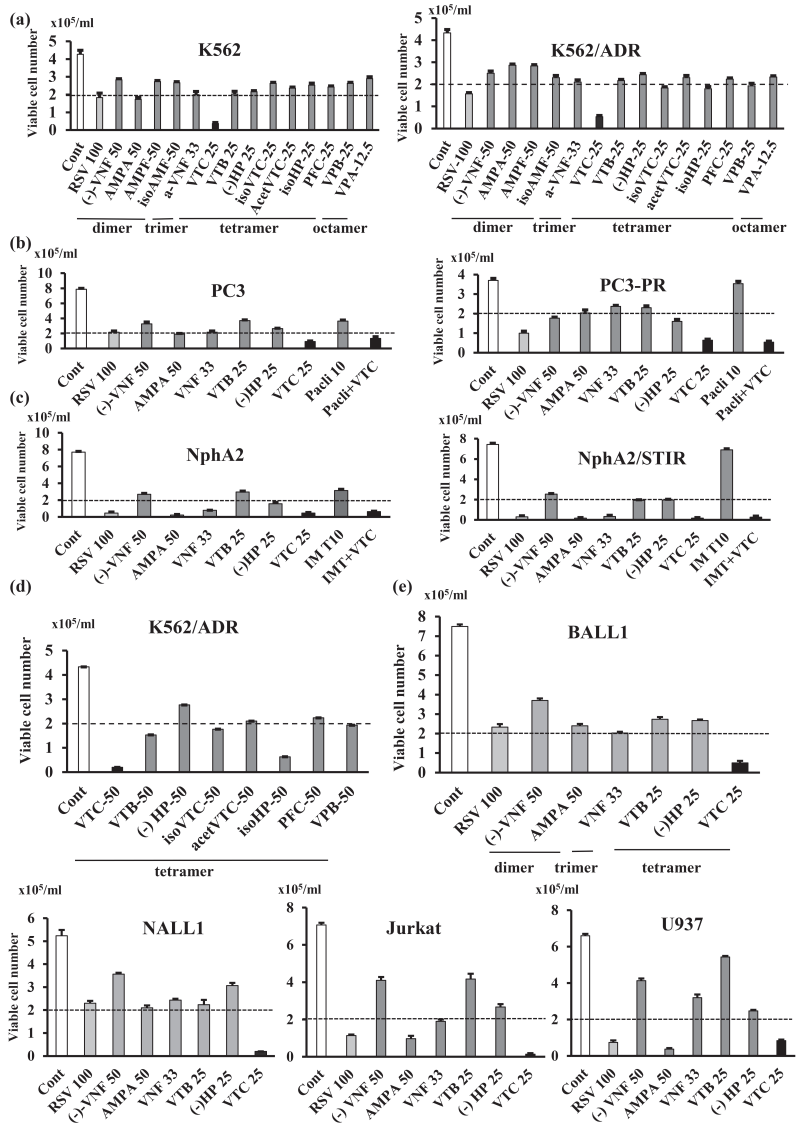


**Fig. 2** Effects of RSV and related oligomers

(a), (b), and (c) Effects of RSV and its oligomers were examined in K562, K562/ADR, PC3, PC3-PR, NphA2, and NphA2/STIR cells. Cells ($2\times10^5$/ml) were treated in triplicate with or without 100 μM RSV (pale gray), 50 μM RSV dimers, 33 μM RSV trimer, 25 μM RSV tetramers (VTC: black), or 12.5 μM RSV octamer. Pacli indicates paclitaxel (20 nM), and IMT indicates imatinib (10 μM ). On day 2, viable cell numbers were counted from triplicate cultures. The mean ± SD was calculated. Representative data are shown from at least three cell culture experiments with the same experimental design. (d) Effects of the RSV tetramer (50 μM) on K562/ADR cells treated with or without 50 μM of eight RSV tetramers in triplicate for 48 hr, and the viable cell numbers were counted. VTC is in black. The mean ± SD is shown. The initial plating cell density was $2\times10^5$/ml (dotted line). Representative data are shown from at least three cell culture experiments with the same experimental design. (e) Effects of RSV oligomers on other leukemia cell lines. In the same way as (a), BALL1, NALL1, Jurkat and U937 cells ($2\times10^5$/ml) were cultured in triplicate with or without RSV (100 μM: pale gray) and 6 major RSV oligomers ((–)-VNF and AMPA: 50 μM, VNF: 33 μM, VTB, (–)-HP and VTC (black): 25 μM) for 48 hr, and viable cell numbers were counted. The mean ± SD was calculated. Representative data are shown from at least three cell culture experiments with the same experimental design.

*Cell survival and proliferation*

Cultures were started in triplicate in 24-well culture plates. Viable cell numbers were counted by trypan blue exclusion using a hemocytometer. The mean ± SD of the viable cell number of each group was calculated. Experiments with the same design were repeated at least three times, and representative results from these repeated experiments are shown in the Figures.

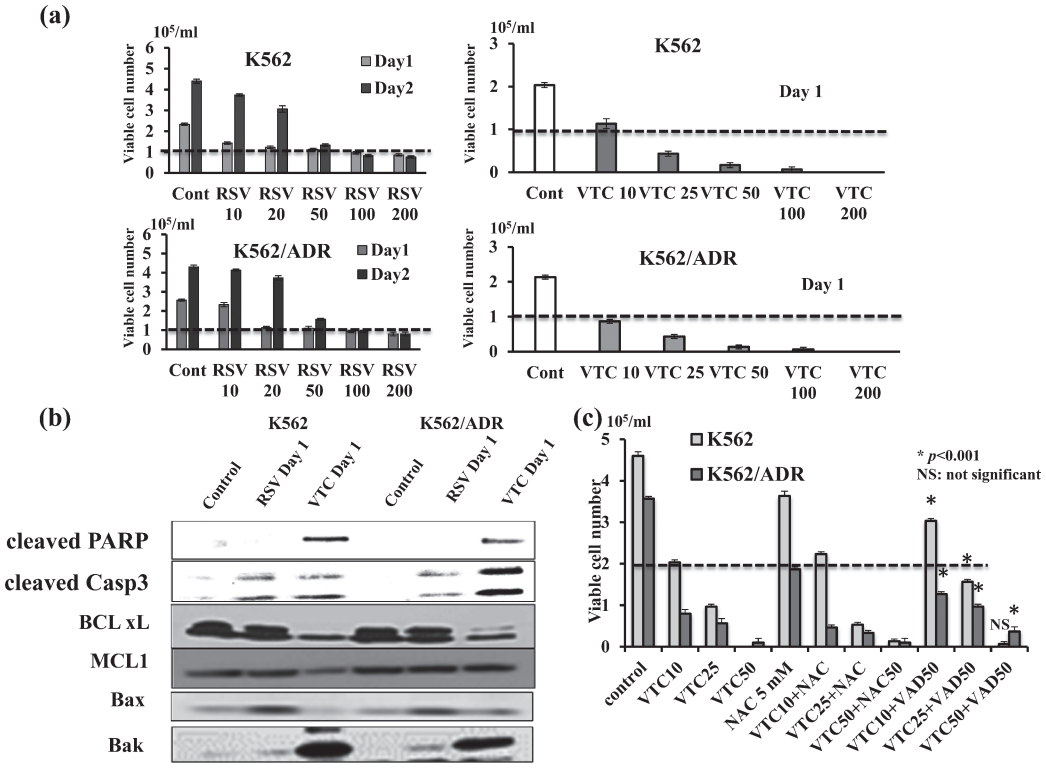


**Fig. 3** Time course of RSV and VTC cytotoxicities

**Fig. 3a:** RSV or VTC (μM concentrations are shown) were added to K562 and K562/ADR cells cultured in triplicate and viable cell numbers were counted on days 1 and 2, respectively. The mean ± SD is shown. The initial plating cell density was $1\times10^5$/ml (dotted line). Representative data are shown from at least three cell culture experiments with the same experimental design.

**Fig. 3b:** Western blotting of apoptosis-related proteins. K562 and K562/ADR cells were treated with RSV (100 μM) or VTC (25 μM) for 24 hr (shown as Control, RSV Day1, and VTC Day1, respectively). Samples were collected, and western blotting was performed according to the Materials and methods. A representative result is shown.

**Fig. 3c:** Effects of NAC and Z-VAD-FMK on VTC cytotoxicity in K562 and K562/ADR cells. Cells ($2\times10^5$/ml) cultured in triplicate were treated with VTC (10, 25, and 50 μM) alone or together with NAC (5 mM) or Z-VAD-FMK (50 μM) for 2 days. Viable cell numbers were counted. The mean ± SD is shown. Statistical significances were analyzed between VTC10 and VTC10+Z-VAD-FMK, between VTC25 and VTC25+Z-VAD-FMK, and between VTC50 and VTC50+Z-VAD-FMK, respectively with one-way factorial analysis of variance and the multiple comparison test (Tukey method).

*May-Giemsa staining*

Cytospin specimens of cells treated with or without RSV or VTC were prepared and stained with May-Giemsa dye.

*ASMase enzyme activity*

ASMase enzyme activity was measured in triplicate according to the method described previously.[14]

*Western blotting*

Western blotting was performed as described previously.[15] Antibodies used are described in Supplementary Table 1. Representative results from at least three independent experiments are shown in the Figures. For bands that exhibited significant changes and were described in the text, respective images were scanned and the band intensity was measured by ImageJ software (https://imagej.nih.gov/ij/index.html). The mean ± SD of the band was calculated from three experiments, and the statistical significance was evaluated using one-way factorial analysis of variance and the multiple comparison test (Dunnett method) (shown in Supplementary Table 2). Western blotting data accompanied with molecular weight marker positions are shown in the Supplementary Figures (Supplementary Fig. 4 for Fig. 3, Supplementary Fig. 5 for Fig. 5 and Supplementary Fig. 6 for Fig. 6).

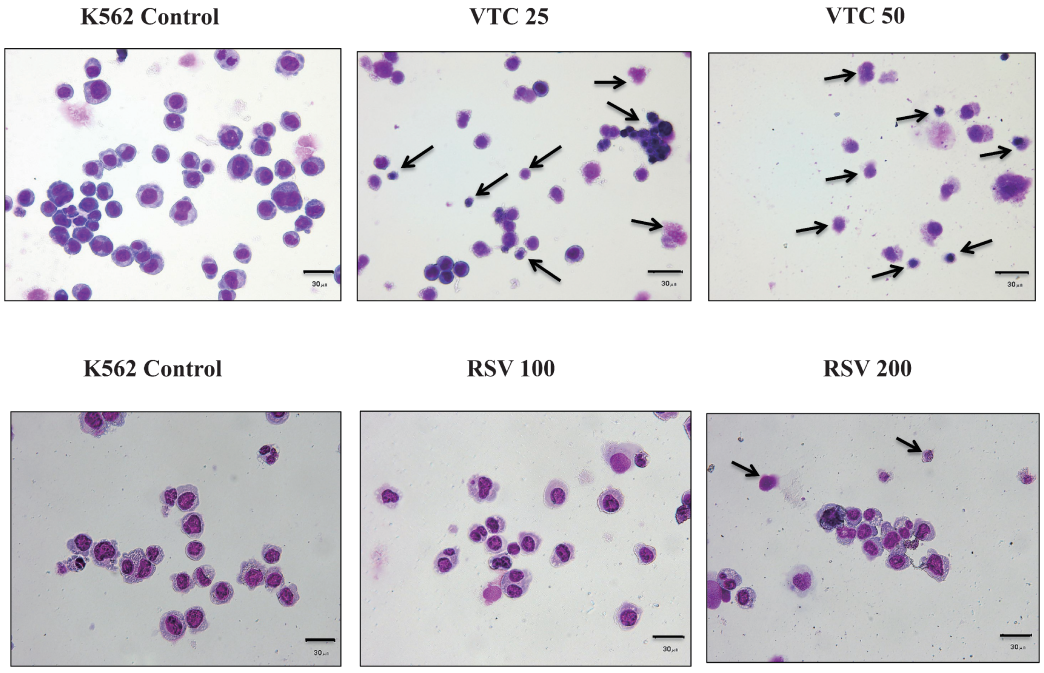


**Fig. 4** Morphological changes of K562 cells induced with RSV and VTC
K562 cells were cultured with VTC or RSV (μM concentrations are shown) for 24 hr, and then cytospin slides were prepared. Cells were stained with May-Giemsa staining as described in the Materials and methods. Arrow indicates apoptotic nuclei or cytoplasm. The solid line at the lower right of the figure = 30 μm.

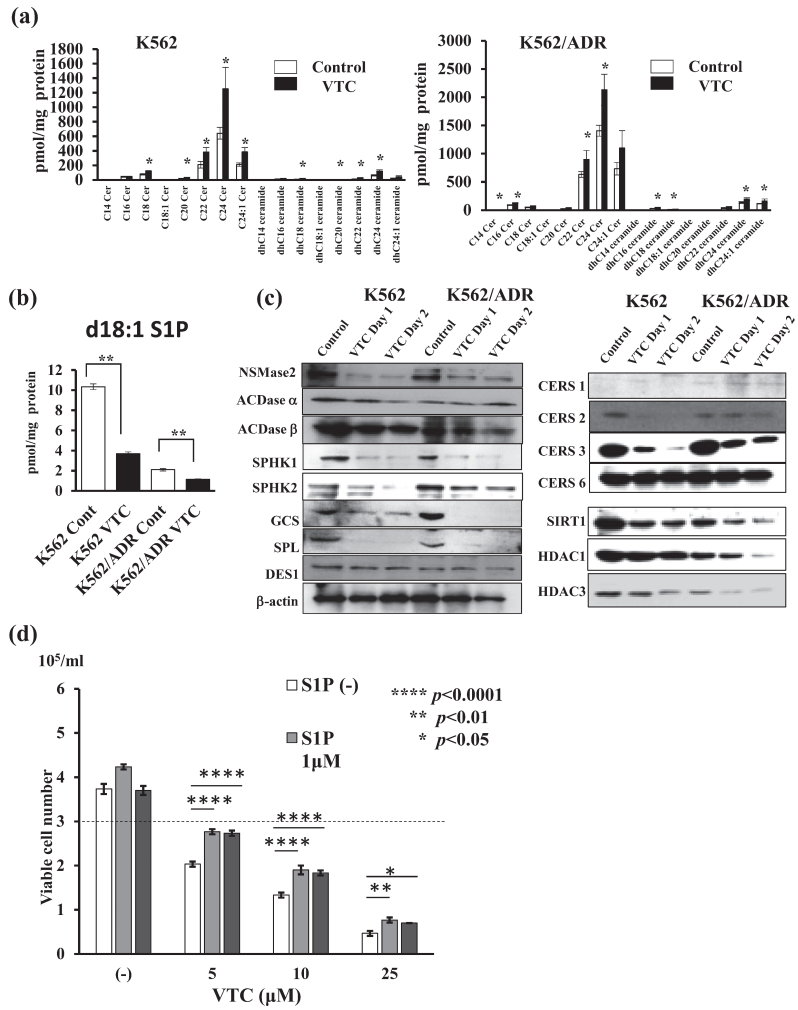


**Fig. 5** Cellular ceramides and S1P levels and related enzyme expressions

(a), (b) K562 and K562/ADR cells were cultured in triplicate with or without VTC (25 μM) treatment for 24 hr. Cellular ceramides and dihydroceramides with different lengths of acyl chain, and S1P were measured by LC/MS-MS according to the Materials and methods. C14 Cer, C16 Cer, C18 Cer, C18:1 Cer, C20 Cer, C22 Cer, C24 Cer, and C24:1 Cer denote (d18:1/14:0), (d18:1/16:0), (d18:1/18:0), (d18:1/18:1), (d18:1/20:0), (d18:1/22:0), (d18:1/24:0), and (d18:1/24:1), respectively. dhC14, dhC16, dhC18, dhC18:1, dhC20, dhC22, dhC24 and dhC24:1 denotes (d18:0/14:0), (d18:0/16:0), (d18:0/18:0), (d18:0/18:1), (d18:0/20:0) (d18:0/22:0), (d18:0/24:0) and (d18:0/24:1), respectively. The mean ± SD is shown. t-test was used to determine statistical significance between C14 ceramide of Control and VTC treated (K562 or K562/ADR) cells, C16 ceramide of Control and VTC treated (K562 or K562/ADR) cells, and C18 ceramide of Control and VTC treated (K562 or K562/ADR) cells. In the same way, all ceramides and dihydroceramides with different lengths of acly chain between Control and VTC-treated cells were analyzed. The statistical significance of cellular S1P between Control and VTC-treated cells was also analyzed by t-test. *p<0.05, **p<0.001. (c) Western blotting of sphingolipid metabolic enzymes. Samples were prepared from K562 and K562/ADR cells with or without VTC treatment for 24 or 48 hr (shown as Control, VTC Day1, and VTC Day2, respectively). Western blotting was performed according to the Materials and methods. (d) Effect of exogenous S1P. K562 cells ($3\times10^5$/ml) were cultured in triplicate in 2% FCS in RPMI1640, and S1P (1 μM and 2 μM) was added. Cells were treated with various doses (μM) of VTC. On day 2, viable cells were counted. The mean ± SD was calculated, and statistical significances were analyzed (Tukey method) between respective doses of VTC with or without S1P addition.

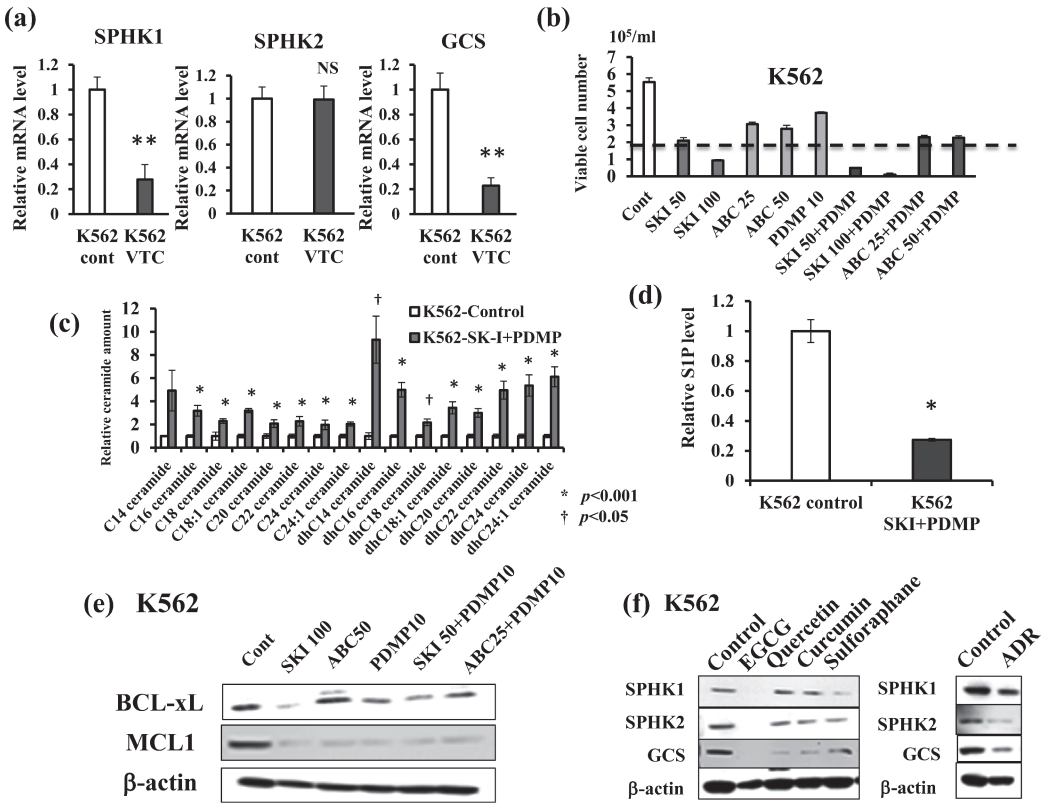


**Fig. 6** Effects of SPHK1/2 and GCS inhibitors and other phytochemicals

(a) QRT-PCR analysis of SPHK1, SPHK2, and GCS in K562 cells. K562 cells were treated in triplicate with or without VTC (25 μM) for 24 hr. QRT-PCR was performed as described in the Materials and methods. The mean ± SD is shown as the summation of two independent experiments, and statistical significances were analyzed by t-test **p<0.0001. NS: not significant. (b) Effects of an SPHK1 inhibitor (SKI, μM), SPHK2 inhibitor (ABC294640, μM), and GCS inhibitor (PDMP, μM) were analyzed in K562 cells cultured in triplicate. Viable cell numbers on Day2 were counted and shown as the mean ± SD. The initial cell density was $2\times10^5$/ml. (c) Cellular ceramides and dihydroceramides were measured in control and SKI (50 μM)+PDMP (10 μM)-treated K562 cells in triplicate (24 hr). Relative ceramide and dihydroceramide levels are shown with ceramide or dihydroceramide levels of control K562 cells regarded as 1.0. The mean ± SD is shown. The statistical significance was analyzed (t-test) as in Fig. 5a. (d) Using the same experimental design as in (c), cellular S1P was measured in control and SKI+PDMP-treated K562 cells. The S1P level in control K562 cells was regarded as 1.0. Statistical significance between control and SKI+PDMP-treated cells was examined as in Fig. 5b. *p<0.005. (e) Anti-apoptotic proteins (BCL-xL, MCL1) of K562 cells treated with or without inhibitors (100 μM SKI, 50 μM ABC294640, 10 μM PDMP, or their combination (μM in the figure) for 48 hr were analyzed by western blotting. β-actin was used as an internal control. (f) Effects of other phytochemicals (100 μM EGCG, 100 μM quercetin, 50 μM curcumin, and 25 μM sulforaphane for 24 hr) on SPHK1, SPHK2, and GCS expressions in K562 cells were analyzed. β-actin was used as an internal control. The effects of ADR (150 nM, 24 hr) on SPHK1, SPHK2 and GCS expressions were examined using K562 cells.

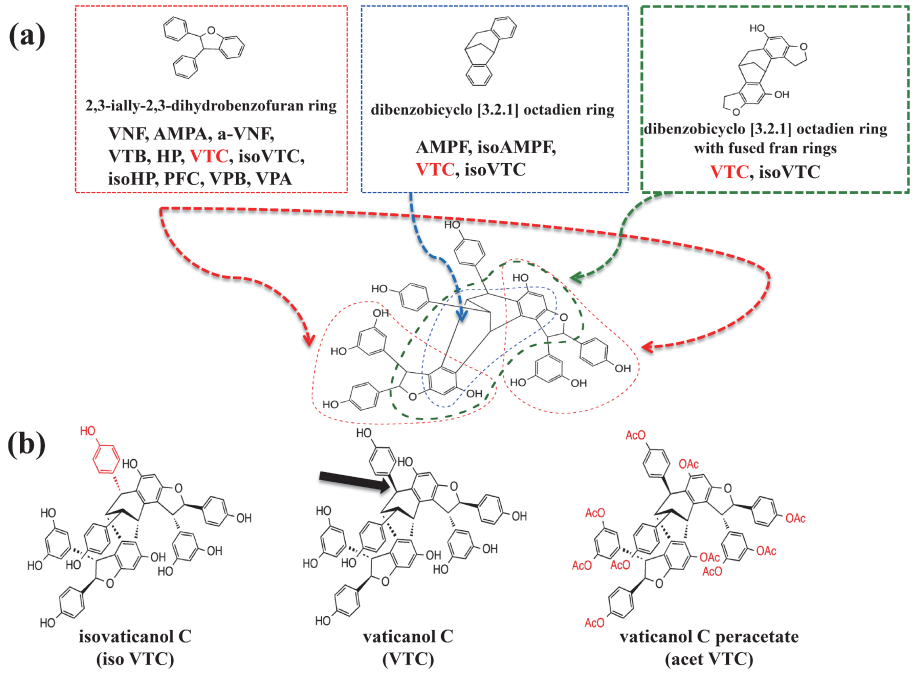


**Fig. 7** Molecular structures of RSV and its oligomers

(a) Molecular structures of RSV oligomers are shown. Three important parts (red, green, and blue boxes) are shown according to the explanation in the Discussion. (b) VTC and two other tetramers, isoVTC and acetVTC (highest structural similarity to VTC), are shown. The region important for cytotoxic function is indicated by a solid arrow (central part) and red color (right and left parts).

**Supplementary Table 1** List of antibodies used for Western blotting experiments

| Target protein | manufacturer | Catalog No | Ab dilution |
|---|---|---|---|
| cleaved PARP | Cell Signaling | # 9532 | 1:1000 |
| cleaved Caspase 3 | Cell Signaling | # 9665 | 1:1000 |
| BCL-xL | Abcam | sc-634 | 1:1000 |
| MCL1 | BD Bioscience | BD-559027 | 1:1000 |
| Bax | BD Bioscience | BD-556467 | 1:1000 |
| Bak | R&D Systems | AF 816 | 1:1000 |
| ACDase α | BD Bioscience | BD-612302 | 1:1000 |
| ACDase β | Santa Cruz | sc-28486 | 1:500 |
| SPHK1 | Cell Signaling | # 3297 | 1:1000 |
| SPHK2 | Santa Cruz | sc-22704 | 1:500 |
| GCS | Santa Cruz | sc-50511 | 1:500 |
| SPL | Santa Cruz | sc-67368 | 1:500 |
| DEGS1 or DES1 | Bioss | bs-4057R | 1:1000 |
| CERS1 | Abnova | PAB18693 | 1:1000 |
| CERS2 | Santa Cruz | sc-100553 | 1:500 |
| CERS3 | Santa Cruz | sc-133725 | 1:500 |
| CERS6 | Abcam | ab56582 | 1:1000 |
| SIRT1 | Santa Cruz | sc-15404 | 1:500 |
| HDAC1 | Santa Cruz | sc-6298 | 1:500 |
| HDAC3 | Santa Cruz | sc-8138 | 1:500 |
| β-actin | Proteintech | 60008-I-Ig | 1:1000 |

**Supplementary Table 2** Western blotting band intensities were measured according to the Materials and methods

**Fig. 3 b**

| | K562 | | | K562/ADR | | |
|---|---|---|---|---|---|---|
| | **Control** | **RSV D1** | **VTC D1** | **Control** | **RSV D1** | **VTC D1** |
| **cleaved PARP** | 1 | 18.81±10.18 * | 20.67±6.42 * | 1 | 23.84±9.60 * | 43.48±13.84 ** |
| **cleaved Caspase 3** | 1 | 8.96±3.86 * | 9.61±3.67 * | 1 | 6.24±4.52 NS | 14.89±7.43 * |
| **BCL-xL** | 1 | 0.85±0.06 NS | 0.35±0.13 *** | 1 | 0.82±0.35 NS | 0.30±0.10 * |
| **Bak** | 1 | 5.29±6.34 NS | 62.80±15.98 *** | 1 | 6.38±3.74 NS | 51.48±20.06 ** |

**Fig. 5 c**

| | K562 | | | K562/ADR | | |
|---|---|---|---|---|---|---|
| | **Control** | **VTC D1** | **VTC D2** | **Control** | **VTC D1** | **VTC D2** |
| **NSMase 2** | 1 | 0.57±0.48 NS | 1.25±1.06 NS | 1 | 0.43±0.18 * | 0.65±0.34 NS |
| **ACDase α** | 1 | 0.72±0.03 NS | 0.94±0.78 NS | 1 | 0.74±0.59 NS | 1.02±0.88 NS |
| **ACDase β** | 1 | 0.79±0.24 NS | 0.86±0.12 NS | 1 | 0.80±0.38 NS | 0.62±0.03 NS |
| **SPHK1** | 1 | 0.20±0.05 *** | 0.18±0.13 *** | 1 | 0.29±0.11 *** | 0.16±0.07 *** |
| **SPHK2** | 1 | 0.34±0.20 ** | 0.14±0.12 *** | 1 | 0.19±0.30 ** | 0.14±0.24 ** |
| **GCS** | 1 | 0.05±0.06 *** | 0.17±0.29 ** | 1 | 0.37±0.33 * | 0.09±0.10 ** |
| **SPL** | 1 | 0.06±0.05 *** | 0.02±0.03 *** | 1 | 0.05±0.05 *** | 0.01±0.01 *** |
| **DES1** | 1 | 1.07±0.47 NS | 0.98±0.49 NS | 1 | 0.92±0.09 NS | 0.71±0.17 * |
| **CERS2** | 1 | 0.15±0.18 *** | 0.01±0.02 *** | 1 | 0.82±0.43 NS | 0.28±0.37 NS |
| **CERS3** | 1 | 0.27±0.05 *** | 0.16±0.11 *** | 1 | 0.16±0.27 ** | 0.12±0.21 ** |

**Fig. 6 e**

| | K562 | | | | | |
|---|---|---|---|---|---|---|
| | **Control** | **SKI** | **ABC** | **PDMP** | **SKI+PDMP** | **ABC+PDMP** |
| **BCL-xL** | 1 | 0.51±0.13 * | 0.94±0.11 NS | 0.74±0.22 NS | 0.76±0.22 NS | 0.78±0.27 NS |
| **MCL1** | 1 | 0.13±0.17 ** | 0.26±0.32 * | 0.48±0.38 NS | 0.23±0.29 * | 0.21±0.13 ** |

**Fig. 6 f**

| | K562 | | | | | |
|---|---|---|---|---|---|---|
| | **Control** | **EGCG** | **Quercetin** | **Curcumin** | **Sulforaphane** | **Adriamycin** |
| **SPHK1** | 1 | 0.08±0.12 * | 0.50±0.34 NS | 0.63±0.15 NS | 0.85±0.66 NS | 0.46±0.14 ** |
| **SPHK2** | 1 | 0.04±0.02 *** | 0.37±0.10 ** | 0.29±0.17 ** | 0.40±0.35 ** | 0.20±0.09 *** |
| **GCS** | 1 | 0 *** | 0.17±0.09 *** | 0.16±0.08 *** | 0.28±0.07 *** | 0.15±0.07 *** |

Band intensity of control K562 or K562/ADR cells was regarded as 1.0, respectively. The mean ± SD was shown and the statistical significances were evaluated between control cells and treated cells using one-way factorial analysis of variance and the multiple comparison test (Dunnet method). Shaded area indicates the statistical significance compared with control cells.

* $p<0.01$, ** $p<0.001$, *** $p<0.0001$, NS: not significant

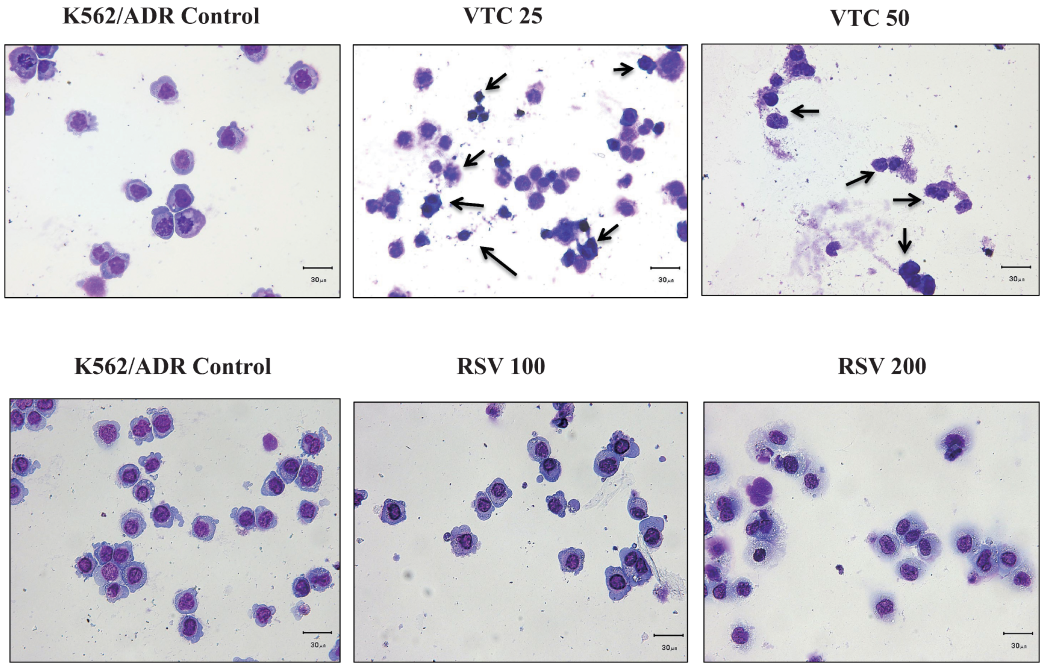


**Supplementary Fig. 1** Morphological change of K562/ADR cells treated with RSV and VTC.
K562/ADR cells were cultured with VTC or RSV (μM concentration as illustrated) for 24 hr, and cytospin-slide was prepared. Cells were stained with May-Giemsa staining as described in the Materials and methods. The solid line at the lower right of the figure was 30 μm. Arrows denote shrunk and concentrated nuclei and cellular fragments in VTC-treated K562/ADR cells.

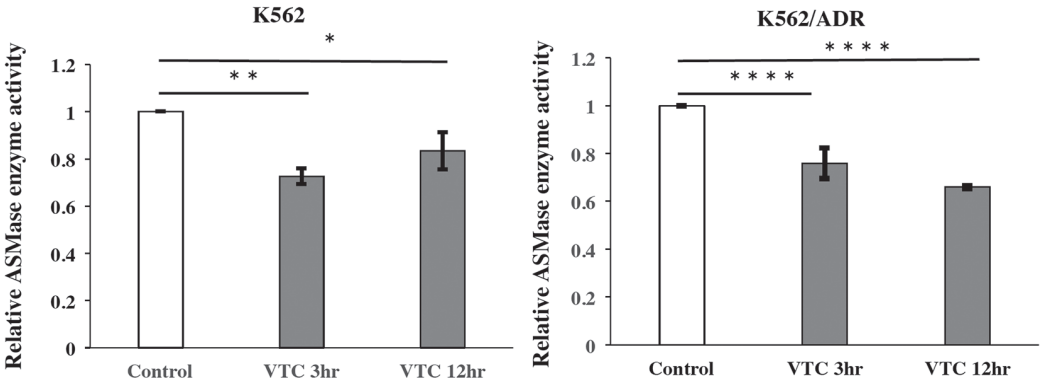


**** $p<0.0001$, ** $p<0.01$, * $p<0.05$

**Supplementary Fig. 2** ASMase enzyme activity: ASMase enzyme activities of control and VTC (25 μM)-treated K562 and K562/ADR cells (3 and 12 hr) in triplicate culture were measured according to the Materials and methods
Statistical significance was analyzed using one-way factorial analysis of variance and the multiple comparison test (Dunnett method) with control cells as the relative activity of 1.0.

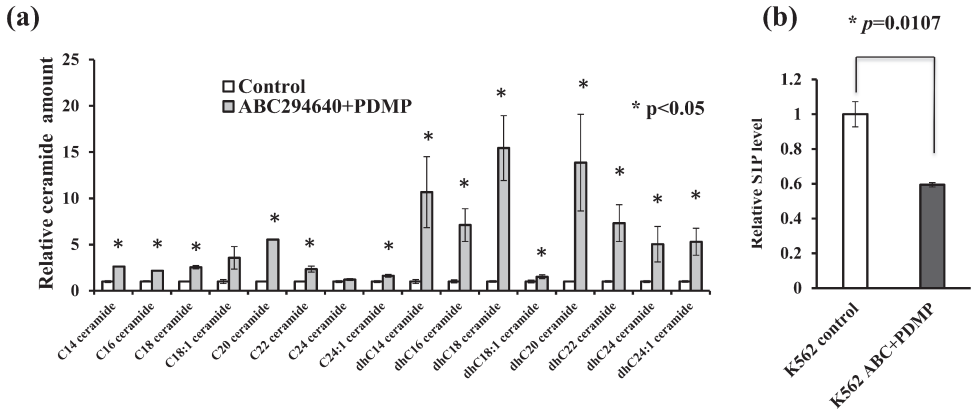


**Supplementary Fig. 3** Effects of ABC294640 (SPHK2 inhibitor) and PDMP (GCS inhibitor) on cellular ceramides and sphingosine-1-phosphate of K562 cells

**Fig. 3a:** In the same way shown in Figures 6c, K562 cells were cultured in triplicate with or without ABC294640 (25 μM) +PDMP (10 μM) treatment for 24 hr. Cellular ceramides and dihydroceramides of control and ABC294640 (25 μM) +PDMP (10 μM) treated K562 cells were measured, and relative amount (the mean ± SD) was illustrated with each ceramide or dihydroceramide level of control K562 cells regarded as 1.0.

The statistical significance was examined using t-test between C14 ceramide of control and ABC294640+PDMP-treated K562 cells, between C16 ceramide of control and ABC294640+PDMP-treated K562 cells, between C18 ceramide of control and ABC294640+PDMP-treated K562 cells, respectively. In the same way, all ceramides and dihydroceramides with different lengths of acly chain between Control and ABC294640+PDMP-treated cells were analyzed. *p<0.05

**Fig. 3b:** In the same experimental design as Supplementary Fig. 3a, relative S1P levels of control and ABC294640+PDMP treated K562 cells were shown with the control K562 cells regarded as 1.0. Statistical significance was analyzed with t-test.

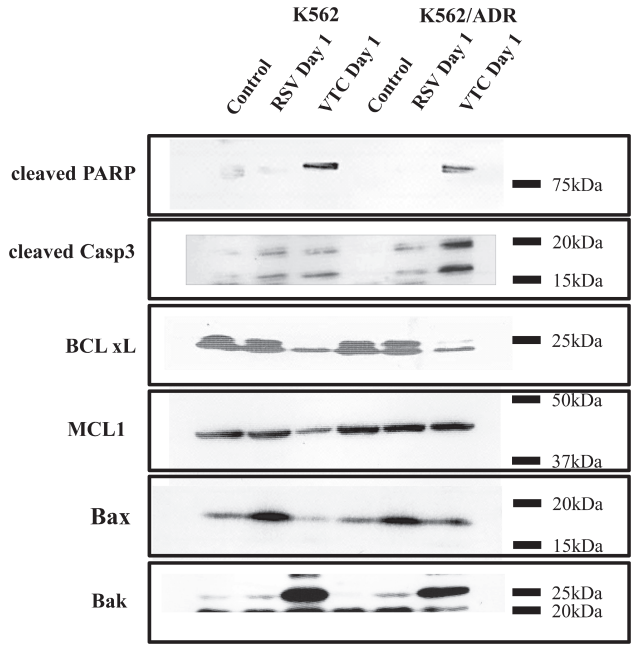


**Supplementary Fig. 4** Western blotting image together with the molecular weight markers (related with Fig. 3b) analyzing apoptosis-related proteins of K562 and K562/ADR cells with or without resveratrol and vaticanol C treatment

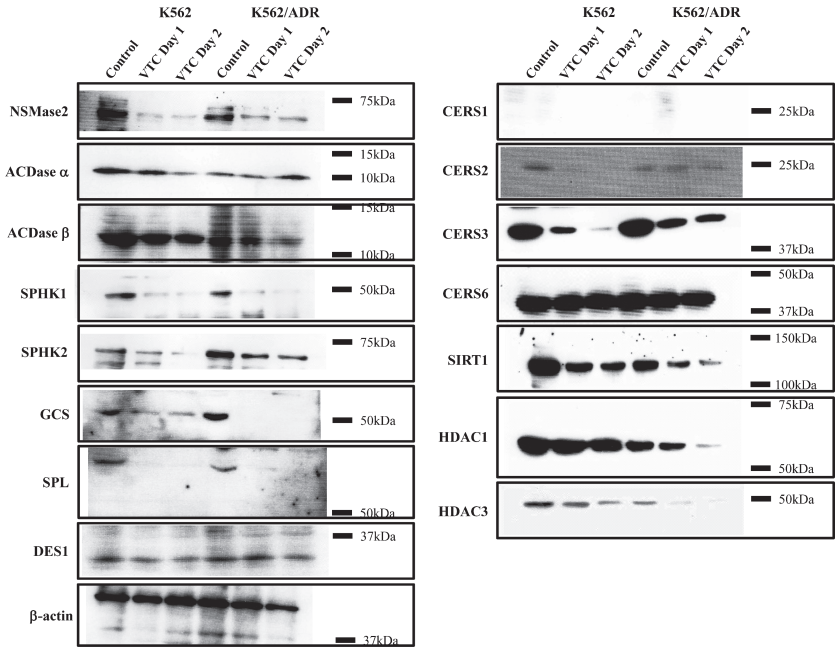


**Supplmentary Fig. 5** Western blotting image together with the molecular weight markers (related with Fig. 5c) analyzing the sphingolipid metabolic enzymes of K562 and K562/ADR cells with or without vaticanol C treatment

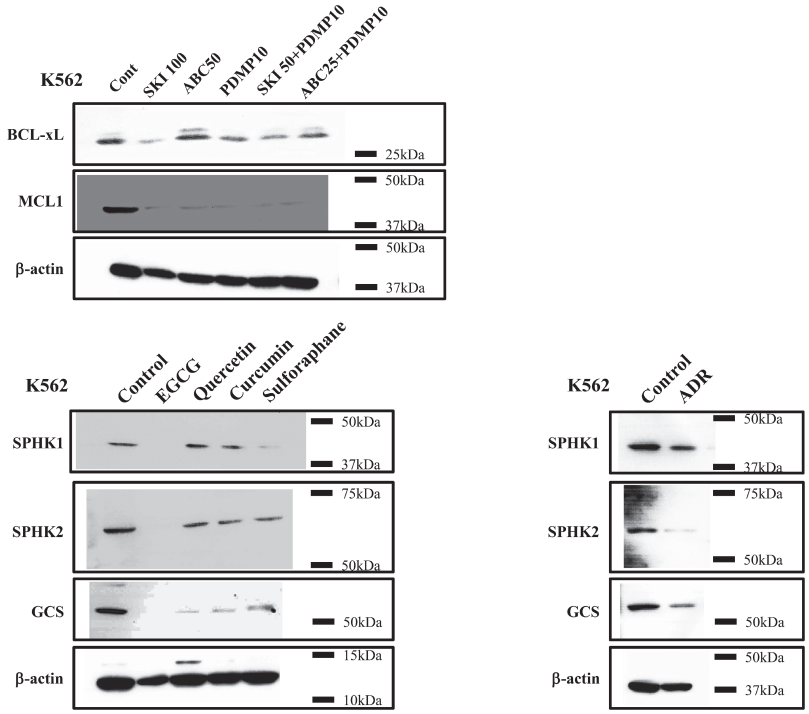


**Supplementary Fig. 6** Western blotting image together with the molecular weight markers (related with Figs. 6e and f) analyzing BCL-xL, MCL1, SPHK1, SPHK2 and GCS proteins of K562 cells treated with various sphingolipid inhibitors, phytochemicals and adriamycin

*QRT-PCR (quantitative reverse transcription-polymerase chain reaction)*

The QRT-PCR procedure and primer sets for SPHK1, SPHK2 and GCS were described previously.[16] First-strand cDNA was prepared from 1 μg RNA using the PrimeScript™ RT reagent Kit (TaKaRa Bio Inc., Otsu, Japan). QRT-PCR was performed with SYBR® Premix ExTaq™ II (TaKaRa). Relative mRNA levels were calculated by the ratio of each mRNA to GAPDH mRNA. GAPDH forward primer: 5′-CAGGAGCGAGATCCCTCCAA-3′; GAPDH reverse primer: 5′-CCCCCTGCAAATGAGCCC-3′.

*Cellular ceramide and S1P*

Cell cultures were performed in triplicate. Cellular ceramides from each sample were prepared as previously described.[17] 18:1-C17:0 ceramide was added prior to lipid extraction as the internal standard. Mass spectrometry analysis was performed with Acquity UltraPerformance LC (Waters, Milford, MA, USA) and QTRAP 4000 LC/MS/MS (AB SCIEX™, Framingham, MA, USA) with an electrospray ionization source in positive ion mode. Chromatographic separation was performed in gradient mode with an ODS column (Cadenza CW-C18, 150 × 3 mm, 3 μM particle size, Imtakt Corp., Portland, OR, USA).[18] The method of sample preparation and quantification of S1P was performed according to the method described previously with d17:1 S1P as an internal control.[19] LC column for S1P measurement was 5C18-AR-II (150 × 2 mm, 5 μM particle size, Nacalai Tesque, Kyoto, Japan). The relative ion abundance of each molecule was calculated from the data of authentic samples. The mean ± SD and statistical significance were calculated for each cellular ceramide with different acyl chain lengths between control and treated cells, and cellular S1P levels between control and treated cells (in Fig. 5, Fig. 6 and Supplementary Fig. 3) were analyzed by *t*-test.

*Statistical analysis*

Statistical significance was analyzed by *t*-test (ceramide and S1P, mRNA level) or one-way factorial analysis of variance and the multiple comparison test (Turkey method for viable cell count and Dunnett's test for the band intensity of western blotting and ASMase activity). All analyses were performed using Prism 6 software (Graphpad; La Jolla, CA, USA). $p<0.05$ was regarded as significant.

## RESULTS

*Cytotoxic effect of VTC*

We analyzed the effects of RSV and its oligomers (Fig. 1) on leukemia (K562 and NphA2) and solid tumor (PC3) cell lines and their anti-cancer drug-resistant sublines. Because the effect of 100 μM RSV on cell growth suppression reached a plateau,[7] we compared the effects of RSV (100 μM), RSV dimers (50 μM), a trimer (33.3 μM), tetramers (25 μM), and octamer (12.5 μM).

All RSV oligomers suppressed the proliferation of K562 cells and K562/ADR cells (Fig. 2a). Among them, VTC exhibited the greatest inhibition and cytotoxicity. Other cell lines and respective anti-cancer drug-resistant sublines (PC3 and PC3-PR, NphA2 and NphA2/STIR) were also very sensitive to VTC (Fig. 2b and 2c). We analyzed 50 μM RSV tetramers (Fig. 2d). VTC at 50 μM was highly cytotoxic among VTC tetramers. Repeating the experiments using other leukemia cell lines (BALL1, NALL1, Jurkat and U937) also revealed the robust cytotoxicity of VTC (Fig. 2e).

*VTC induces more rapid cytotoxicity than RSV*

We focused on the cytotoxic effect of VTC in comparison with RSV. RSV suppressed K562 and K562/ADR cell proliferation in a dose-dependent manner, but cell death induction required a higher concentration and was slow. In contrast, viable cell numbers were more rapidly decreased by VTC (Fig. 3a). The $IC_{50}$ after VTC and RSV treatment (24 h) against K562 cells and K562/ADR cells was 25 μM and 350 μM, respectively. Thus, the cytotoxic efficiency of VTC was at least 10 times greater than that of RSV.

VTC (25 μM) induced cleaved poly ADP-ribose polymerase (PARP) and cleaved caspase 3 (Fig. 3b). VTC reduced the anti-apoptotic protein, BCL-xL, and increased the pro-apoptotic protein, Bak. Because NAC (anti-ROS activity) itself inhibited cell proliferation, we could not evaluate the effect of NAC. However, Z-VAD-FMK (a pan-caspase 3 inhibitor) significantly attenuated VTC-induced cell death, suggesting that VTC induced apoptotic cell death (Fig. 3c). Morphological analysis with May-Giemsa staining of K562 and K562/ADR cells after VTC (25 μM and 50 μM for 24 h) treatment showed many shrunk and concentrated nuclei and cellular fragments (arrows) in VTC-treated cells, whereas in RSV 200 (200 μM)-treated K562 cells, fewer shrunk nuclei or cytoplasmic debris were observed (Fig. 4 and Supplementary Fig. 1).

*VTC increases cellular ceramides and decreases S1P*

VTC (25 μM) increased cellular ceramides (almost all ceramides and dihydroceramides with different acyl chain lengths) and decreased cellular S1P in K562 and K562/ADR cells (Fig. 5a and b).

*VTC decreases SPHK1, SPHK2, and GCS expressions*

We previously reported that RSV increased ASMase mRNA and enzyme activity.[7] However, VTC did not increase ASMase enzyme activity (Supplementary Fig. 2) or neutral sphingomyelinase 2 (NSMase2) expression (Fig. 5c). VTC inhibited the expressions of SPHK1, SPHK2, GCS, and sphingosine 1-phosphate lyase (SPL), but not the expressions of two acid ceramidase (ACDase) subunits, α and β.[20] Ceramide synthase 1 (CERS1) was very low in K562 and K562/ADR cells and CERS2 and CERS3 were decreased by VTC. Dihydroceramide desaturase (DES1) that metabolizes dihydroceramide to ceramide was not suppressed in any group except VTC-treated K562/ADR cells on Day 2 (Fig. 5c).

RSV was reported to activate SIRT1, a class III HDAC (histone deacetylase).[21] However, Sirtuin 1 (SIRT1) and other HDACs (HDAC1 and HDAC3) were moderately decreased by VTC. Moreover, exogenous S1P addition reduced VTC cytotoxicity significantly (Fig. 5d).

QRT-PCR analysis showed that SPHK1 and GCS, but not SPHK2, were decreased by VTC (Fig. 6a), suggesting the transcriptional (SPHK1 and GCS) and post-transcriptional regulation (SPHK2) of these enzymes in K562 cells.

*Inhibitors of SPHK and GCS and other phytochemicals*

To examine the relevance of VTC-induced changes in sphingolipid metabolic enzyme expression, chemical inhibitors of SPHK1, SPHK2 and GCS were examined. In separate experiments, the effects of PDMP (a GCS inhibitor)[22] and GT-11 (a DES1 inhibitor)[23] were examined, and shown to inhibit K562 cell proliferation mildly and not induce apoptosis (Fig. 6b and data not shown). In experiments with SPHK1 or SPHK2 inhibitors, GT-11 was not included because of the DES1 inhibitory activity of SKI (a SPHK1 inhibitor) and ABC294640 (a SPHK2 inhibitor).[24] SKI markedly inhibited K562 cell proliferation, and a high concentration induced cytotoxicity (Fig. 6b). SKI+PDMP induced remarkable cytotoxicity. In contrast, ABC294640 + PDMP induced milder growth suppression.

SKI + PDMP increased cellular ceramides and dihydroceramides with different acyl chain lengths, and decreased S1P in K562 cells (Fig. 6c and d). ABC294640 + PDMP induced similar changes (Supplementary Fig. 3).

SKI (100 μM) suppressed BCL-xL and MCL1 expressions. Combinations of SKI (50 μM) + PDMP (10 μM), and ABC (25 μM) + PDMP (10 μM), also decreased MCL1 expression significantly; however, BCL-xL inhibition by this combination treatment was mild and not statistically significant (Fig. 6e).

To examine whether sphingolipid enzyme modulation was specific to VTC-induced cell death, the effects of other phytochemicals on SPHK1, SPHK2, and GCS expressions were examined (Fig. 6f). EGCG significantly inhibited SPHK1 and SPHK2 and GCS expression. Interestingly, ADR, an anti-cancer drug frequently used for various cancers, induced changes in K562 cells similar to VTC or EGCG.

## DISCUSSION

Since the discovery of the carcinogenesis-preventing effect of RSV,[3] many studies have reported its anti-proliferative activity in mouse and human cancer cells and *in vivo* or *in vitro* cancer models.[25] RSV is effective in anti-cancer drug-resistant cells by sensitizing them to anti-cancer drugs.[26]

However, RSV has a poor pharmacokinetic profile. It is rapidly metabolized in the body by sulfation and glucuronidation, thereby reducing its bioavailability. The half-lives of RSV and total RSV metabolites are 8–14 min and 9 hr, respectively. Thus, it is less likely that RSV reaches a serum concentration above 1 μM from daily components or 10 μM from RSV supplement consumption.[27] Higher doses of RSV such as 250 mg resulted in plasma levels of 2–18 μM,[28] which is still insufficient to induce cytotoxicity *in vitro*.

To overcome this drawback, novel RSV analogs with higher bioavailability are a candidate strategy. RSV oligomers including VTC have been reported to exhibit robust cytotoxic activity by us and others.[8,29] RSV oligomers are expected to reduce the *in vivo* concentration required for cytotoxicity compared with RSV. The rapid and strong cytotoxicity of VTC (Fig. 2 and Fig. 3) suggests VTC induced apoptosis. The $IC_{50}$ of VTC and RSV indicates VTC was more effective than RSV in K562 cells. Intriguingly, VTC was highly cytotoxic in various anti-cancer drug-resistant cells possessing different resistance mechanisms (Figs. 2 and 3), which is promising for future clinical use.

VTC decreased cellular S1P and increased cellular ceramides including dihydroceramides (Fig. 5a and b), which might be a cause of VTC-induced apoptosis. These data are consistent with our recent report showing the effect of RSV on ceramide accumulation.[7] However, VTC affected multiple sphingolipid metabolic enzymes other than ASMase (Fig. 5c). Based on the sphingolipid rheostat, we focused on SPHK1, SPHK2, and GCS, whose combination was expected to decrease cellular S1P and increase cellular ceramides. VTC decreased SPHK1 and GCS, but not SPHK2 mRNA expression (Fig. 6a), indicating heterogeneous regulatory mechanisms of VTC.

RSV induced ASMase transcription by increasing EGR transcription factors followed by an increase in cellular ceramide,[7] whereas VTC suppressed SPHK1 and GCS transcription leading to increased cellular ceramides and decreased S1P, suggesting different mechanisms of RSV and VTC involved in the increase of cellular ceramides. Similarly, an RSV dimer, balanocarpol, inhibited SPHK1 activity and expression to a higher degree than RSV[30]; however, high concentrations (100 μM) suppressed total cellular DNA synthesis and SPHK1 protein expression.

The combination of SKI + PDMP increased ceramides and dihydroceramides, and suppressed S1P in K562 cells (Figs. 6c and Supplementary Fig. 3), consistent with recent reports showing

the potent DES1 inhibitory action of SPHK inhibitors.[24] DES1 suppression is suspected to be responsible for the increase in dihydroceramides. Although VTC increased cellular dihydroceramides in K562 and K562/ADR cells, DES1 expression was not significantly decreased by VTC except in VTC-treated K562/ADR cells on Day 2 (Fig. 5c). However, DES1 activation by palmitic acid activated DES1 leading to cell death,[31] and DES1 ablation conferred resistance to etoposide-induced apoptosis.[32] Thus, the effects of DES1 inhibition are variable depending on the cellular context and degree of inhibition.[33] The role of DES1 in VTC treatment remains to be determined and further analysis is needed.

Increased SPHK1[34] and GCS[35] were reported in anti-cancer drug-resistant cancer cells. In such cancer cells, SPHK1 and/or GCS overexpression is expected to modulate the sphingolipid rheostat (decrease of S1P and increase of ceramide) and to support cancer cell survival and resistance against extracellular stress such as anti-cancer drugs.

In the present study, we used K562 and NphA2, both of which are BCR/ABL positive leukemia cells. SPHK1 expression was upregulated by BCR/ABL translocation[36] and signaling through the S1P2 receptor by S1P stabilized oncogenic BCR/ABL proteins.[37] Although we did not provide direct evidence for a relationship between VTC treatment and S1P receptor signaling, the results of exogenous S1P addition (Fig. 5d) supported the involvement of S1P/S1P receptor signaling in K562 cells. In contrast, GCS overexpression increased cellular glucosylceramide[38] and decreased ceramide,[39] also leading to the modulation of the sphingolipid rheostat. Indeed, a GCS inhibitor PDMP sensitized imatinib-resistant T315 mutation positive CML cells.[40]

However, the role of SPHK2 in the cancer field is unclear. In the early period of SPHK2 research, the overexpression of SPHK2 inhibited cell proliferation and promoted apoptosis.[41] In contrast, ABC294640 (an SPHK2 inhibitor) inhibited the growth of different tumor cell lines *in vivo*, and had a chemo-sensitizing effect.[42] Our results confirmed the inhibitory effect of ABC294640 on malignant cell growth and survival.

Because of difficulties using multiple siRNAs simultaneously, we used chemical inhibitors. The combination of SPHK1 and GCS inhibitors exhibited remarkable cytotoxicity and showed similar sphingolipid rheostat modulation as that of VTC (Fig. 6b). In addition to VTC, the decreased expressions of these sphingolipid metabolic enzymes were observed using another phytochemical, EGCG, and an anti-cancer drug, ADR (Figs. 4c and 5d), suggesting the same cytotoxic mechanism in leukemia cells (e.g. affecting the sphingolipid rheostat).

Although 14 oligomers with hydroxy groups have one or more common fused ring(s), [2,3-diallyl-2,3-dihydrobenzofuran ring(s)] (***red box***, VNF, AMPA, α-VNF, VTB, HP, ***VTC***, isoVTC, isoHP, PFC, VPB, and VPA) and dibenzobicyclo [3.2.1] octadiene ring (***blue box***, AMPF, isoAMPF, ***VTC***, and isoVTC) (Fig. 7a), only VTC showed a robust cytotoxic effect. Considering the molecular structures, a backbone with two furan rings (***red box***) fused to a central bicyclo ring (***green box***) was crucial to demonstrate VTC-induced cytotoxic effects.

Of note, by comparing two similar tetramers, (isoVTC and acetVTC) with VTC, the orientation of a 4-hydroxybenzene ring attached to the bicyclo ring [shown as **the solid arrow** (middle) compared with the red color (left) of Fig. 7b] was important for the cytotoxic action of VTC, considering the diminished cytotoxicity of isoVTC. Moreover, decreased cytotoxicity was demonstrated by peracetate of VTC (acetVTC: **red AcO** in the right compared with VTC, Fig. 7b), showing the importance of the hydroxyl group for its cytotoxicity, which was similar to RSV and its analog.[43] These characteristics are important for the future translational research of VTC as a prototype molecule.

In summary, our results suggest that VTC exhibited robust cytotoxicity against leukemia and solid tumors with or without various anti-cancer drug resistance and that VTC might be a promising prototype for translational research.

## ACKNOWLEDGEMENT

We thank Edanz Group (www.edanzediting.com/ac) for editing a draft of this manuscript.

## CONFLICT OF INTEREST STATEMENT

All authors disclose no actual or potential conflict of interest including any financial, personal or other relationships with other people or organization.

## REFERENCES

1. Athar M, Back JH, Kopelovich L, Bickers DR, Kim AL. Multiple molecular targets of resveratrol: anti-carcinogenic mechanisms. *Arch Biochem Biophys*. 2009;486(2):95–102.
2. Kulkarni SS, Canto C. The molecular targets of resveratrol. *Biochim Biophys Acta*. 2015;1852(6):1114–1123.
3. Jang M, Cai L, Udeani GO, et al. Cancer chemopreventive activity of resveratrol, a natural product derived from grapes. *Science*. 1997;275(5297):218–220.
4. Hadi SM, Asad SF, Singh S, Ahmad A. Putative mechanism for anticancer and apoptosis-inducing properties of plant-derived polyphenolic compounds. *IUBMB life*. 2000;50(3):167–171.
5. Ogretmen B. Sphingolipid metabolism in cancer signalling and therapy. *Nat Rev Cancer*. 2018;18(1):33–50.
6. Edsall LC, Van Brocklyn JR, Cuvillier O, Kleuser B, Spiegel S. N,N-Dimethylsphingosine is a potent competitive inhibitor of sphingosine kinase but not of protein kinase C: modulation of cellular levels of sphingosine 1-phosphate and ceramide. *Biochemistry*. 1998;37(37):12892–12898.
7. Mizutani N, Omori Y, Kawamoto Y, et al. Resveratrol-induced transcriptional up-regulation of ASMase (SMPD1) of human leukemia and cancer cells. *Biochem Biophys Res Commun*. 2016;470(4):851–856.
8. Ito T, Akao Y, Yi H, et al. Antitumor effect of resveratrol oligomers against human cancer cell lines and the molecular mechanism of apoptosis induced by vaticanol C. *Carcinogenesis*. 2003;24(9):1489–1497.
9. Nishida Y, Mizutani N, Inoue M, et al. Phosphorylated Sp1 is the regulator of DNA-PKcs and DNA ligase IV transcription of daunorubicin-resistant leukemia cell lines. *Biochim Biophys Acta*. 2014;1839(4):265–274.
10. Sobue S, Mizutani N, Aoyama Y, et al. Mechanism of paclitaxel resistance in a human prostate cancer cell line, PC3-PR, and its sensitization by cabazitaxel. *Biochem Biophys Res Commun*. 2016;479(4):808–813.
11. Inoue C, Sobue S, Aoyama Y, et al. BCL2 inhibitor ABT-199 and JNK inhibitor SP600125 exhibit synergistic cytotoxicity against imatinib-resistant Ph+ ALL cells. *Biochem Biophys Rep*. 2018;15:69–75.
12. Sobue S, Nemoto S, Murakami M, et al. Implications of sphingosine kinase 1 expression level for the cellular sphingolipid rheostat: relevance as a marker for daunorubicin sensitivity of leukemia cells. *Int J Hematol*. 2008;87(3):266–275.
13. Triola G, Fabrias G, Casas J, Llebaria A. Synthesis of cyclopropene analogues of ceramide and their effect on dihydroceramide desaturase. *J Org Chem*. 2003;68(26):9924–9932.
14. Ito H, Murakami M, Furuhata A, et al. Transcriptional regulation of neutral sphingomyelinase 2 gene expression of a human breast cancer cell line, MCF-7, induced by the anti-cancer drug, daunorubicin. *Biochim Biophys Acta*. 2009;1789(11-12):681–690.
15. Furuhata A, Kimura A, Shide K, et al. p27 deregulation by Skp2 overexpression induced by the JAK2V617 mutation. *Biochem Biophys Res Commun*. 2009;383(4):411–416.
16. Sobue S, Iwasaki T, Sugisaki C, et al. Quantitative RT-PCR analysis of sphingolipid metabolic enzymes in acute leukemia and myelodysplastic syndromes. *Leukemia*. 2006;20(11):2042–2046.
17. Tanaka K, Tamiya-Koizumi K, Hagiwara K, et al. Role of down-regulated neutral ceramidase during all-trans retinoic acid-induced neuronal differentiation in SH-SY5Y neuroblastoma cells. *J Biochem*. 2012;151(6):611–620.
18. Kasumov T, Huang H, Chung YM, Zhang R, McCullough AJ, Kirwan JP. Quantification of ceramide species in biological samples by liquid chromatography electrospray ionization tandem mass spectrometry. *Anal Biochem*. 2010;401(1):154–161.
19. Nakanishi H, Ogiso H, Taguchi R. Qualitative and quantitative analyses of phospholipids by LC-MS for lipidomics. *Methods Mol Biol*. 2009;579:287–313.
20. Bernardo K, Hurwitz R, Zenk T, et al. Purification, characterization, and biosynthesis of human acid ceramidase. *J Biol Chem*. 1995;270(19):11098–11102.

21. Yun JM, Chien A, Jialal I, Devaraj S. Resveratrol up-regulates SIRT1 and inhibits cellular oxidative stress in the diabetic milieu: mechanistic insights. *J Nutr Biochem*. 2012;23(7):699–705.
22. Baran Y, Bielawski J, Gunduz U, Ogretmen B. Targeting glucosylceramide synthase sensitizes imatinib-resistant chronic myeloid leukemia cells via endogenous ceramide accumulation. *J Cancer Res Clin Oncol*. 2011;137(10):1535–1544.
23. Triola G, Fabrias G, Dragusin M, et al. Specificity of the dihydroceramide desaturase inhibitor N-[(1R,2S)-2-hydroxy-1-hydroxymethyl-2-(2-tridecyl-1-cyclopropenyl)ethyl]octanami de (GT11) in primary cultured cerebellar neurons. *Mol Pharmacol*. 2004;66(6):1671–1678.
24. McNaughton M, Pitman M, Pitson SM, Pyne NJ, Pyne S. Proteasomal degradation of sphingosine kinase 1 and inhibition of dihydroceramide desaturase by the sphingosine kinase inhibitors, SKi or ABC294640, induces growth arrest in androgen-independent LNCaP-AI prostate cancer cells. *Oncotarget*. 2016;7(13):16663–16675.
25. Fukui M, Yamabe N, Zhu BT. Resveratrol attenuates the anticancer efficacy of paclitaxel in human breast cancer cells in vitro and in vivo. *Eur J Cancer*. 2010;46(10):1882–1891.
26. Mondal A, Bennett LL. Resveratrol enhances the efficacy of sorafenib mediated apoptosis in human breast cancer MCF7 cells through ROS, cell cycle inhibition, caspase 3 and PARP cleavage. *Biomed Pharmacother*. 2016;84:1906–1914.
27. Baur JA, Sinclair DA. Therapeutic potential of resveratrol: the in vivo evidence. *Nat Rev Drug Discov*. 2006;5(6):493–506.
28. Wightman EL, Reay JL, Haskell CF, Williamson G, Dew TP, Kennedy DO. Effects of resveratrol alone or in combination with piperine on cerebral blood flow parameters and cognitive performance in human subjects: a randomised, double-blind, placebo-controlled, cross-over investigation. *Br J Nutr*. 2014;112(2):203–213.
29. Colin D, Gimazane A, Lizard G, et al. Effects of resveratrol analogs on cell cycle progression, cell cycle associated proteins and 5fluoro-uracil sensitivity in human derived colon cancer cells. *Int J Cancer*. 2009;124(12):2780–2788.
30. Lim KG, Gray AI, Pyne S, Pyne NJ. Resveratrol dimers are novel sphingosine kinase 1 inhibitors and affect sphingosine kinase 1 expression and cancer cell growth and survival. *Br J Pharmacol*. 2012;166(5):1605–1616.
31. Zhu Q, Yang J, Zhu R, et al. Dihydroceramide-desaturase-1-mediated caspase 9 activation through ceramide plays a pivotal role in palmitic acid-induced HepG2 cell apoptosis. *Apoptosis*. 2016;21(9):1033–1044.
32. Siddique MM, Bikman BT, Wang L, et al. Ablation of dihydroceramide desaturase confers resistance to etoposide-induced apoptosis in vitro. *PLoS One*. 2012;7(9):e44042.
33. Casasampere M, Ordonez YF, Pou A, Casas J. Inhibitors of dihydroceramide desaturase 1: therapeutic agents and pharmacological tools to decipher the role of dihydroceramides in cell biology. *Chem Phys Lipids*. 2016;197:33–44.
34. Zhang Y, Wang Y, Wan Z, Liu S, Cao Y, Zeng Z. Sphingosine kinase 1 and cancer: a systematic review and meta-analysis. *PLoS One*. 2014;9(2):e90362.
35. Gouaze V, Liu YY, Prickett CS, Yu JY, Giuliano AE, Cabot MC. Glucosylceramide synthase blockade down-regulates P-glycoprotein and resensitizes multidrug-resistant breast cancer cells to anticancer drugs. *Cancer Res*. 2005;65(9):3861–3867.
36. Li QF, Huang WR, Duan HF, Wang H, Wu CT, Wang LS. Sphingosine kinase-1 mediates BCR/ABL-induced upregulation of Mcl-1 in chronic myeloid leukemia cells. *Oncogene*. 2007;26(57):7904–7908.
37. Salas A, Ponnusamy S, Senkal CE, et al. Sphingosine kinase-1 and sphingosine 1-phosphate receptor 2 mediate Bcr-Abl1 stability and drug resistance by modulation of protein phosphatase 2A. *Blood*. 2011;117(22):5941–5952.
38. Lavie Y, Cao H, Bursten SL, Giuliano AE, Cabot MC. Accumulation of glucosylceramides in multidrug-resistant cancer cells. *J Biol Chem*. 1996;271(32):19530–19536.
39. Itoh M, Kitano T, Watanabe M, et al. Possible role of ceramide as an indicator of chemoresistance: decrease of the ceramide content via activation of glucosylceramide synthase and sphingomyelin synthase in chemoresistant leukemia. *Clin Cancer Res*. 2003;9(1):415–423.
40. Huang WC, Tsai CC, Chen CL, et al. Glucosylceramide synthase inhibitor PDMP sensitizes chronic myeloid leukemia T315I mutant to Bcr-Abl inhibitor and cooperatively induces glycogen synthase kinase-3-regulated apoptosis. *FASEB J*. 2011;25(10):3661–3673.
41. Igarashi N, Okada T, Hayashi S, Fujita T, Jahangeer S, Nakamura S. Sphingosine kinase 2 is a nuclear protein and inhibits DNA synthesis. *J Biol Chem*. 2003;278(47):46832–46839.
42. White MD, Chan L, Antoon JW, Beckman BS. Targeting ovarian cancer and chemoresistance through selective inhibition of sphingosine kinase-2 with ABC294640. *Anticancer Res*. 2013;33(9):3573–3579.

43. Ashikawa K, Majumdar S, Banerjee S, Bharti AC, Shishodia S, Aggarwal BB. Piceatannol inhibits TNF-induced NF-kappaB activation and NF-kappaB-mediated gene expression through suppression of IkappaBalpha kinase and p65 phosphorylation. *J Immunol.* 2002;169(11):6490–6497.